Science Advances
AAAS

Supplementary Materials for

Glucose-sensing glucagon-like peptide-1 receptor neurons in the dorsomedial hypothalamus regulate glucose metabolism

Zhaohuan Huang *et al.*

Corresponding author: Ji Liu, geeliu6@gmail.com

Sci. Adv. **8**, eabn5345 (2022)
DOI: 10.1126/sciadv.abn5345

This PDF file includes:

Figs. S1 to S6

Fig. S1.

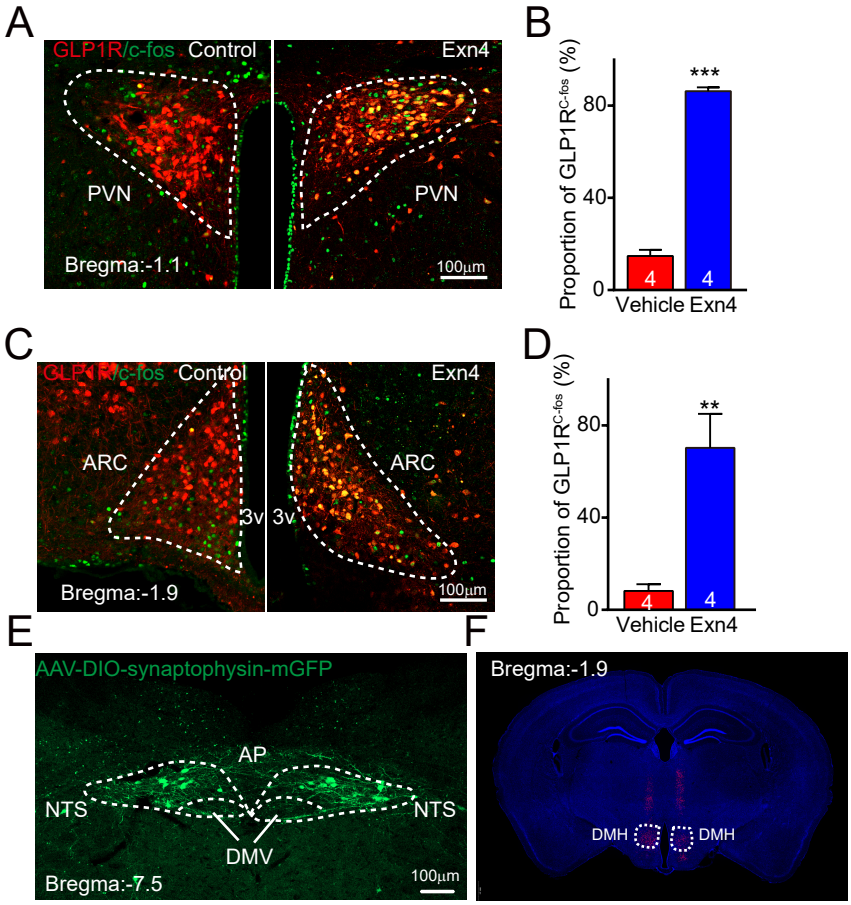

Figure S1| A, ICV Exn4 induced increased c-Fos expression in the GLP-1R neurons of paraventricular nucleus of hypothalamus (PVN) in the *GLP-1R-Cre* mice; **B,** Quantification of c-Fos positive cells ration (relative to total GLP-1R neurons), ***p<0.001 (t-test); **C,** ICV Exn4 induced increased c-Fos expression in the GLP-1R neurons of arcuate nucleus (ARC) in the *GLP-1R-Cre* mice; **D,** Quantification of c-Fos positive cells ration (relative to total GLP -1R neurons), **p<0.01 (t-test); **E,** AAV-DIO-synaptophysin-mGFP mediated GFP expression in the NTS of *Gcg-Cre* mice. **F,** To verify the injection site for retro-AAV-DIO-GFP in the DMH of *Gcg-Cre* mice, we mixed with AAV-mCherry during injection, which was showed by the representative brain slice. n numbers are indicated in each panel.

Fig. S2.

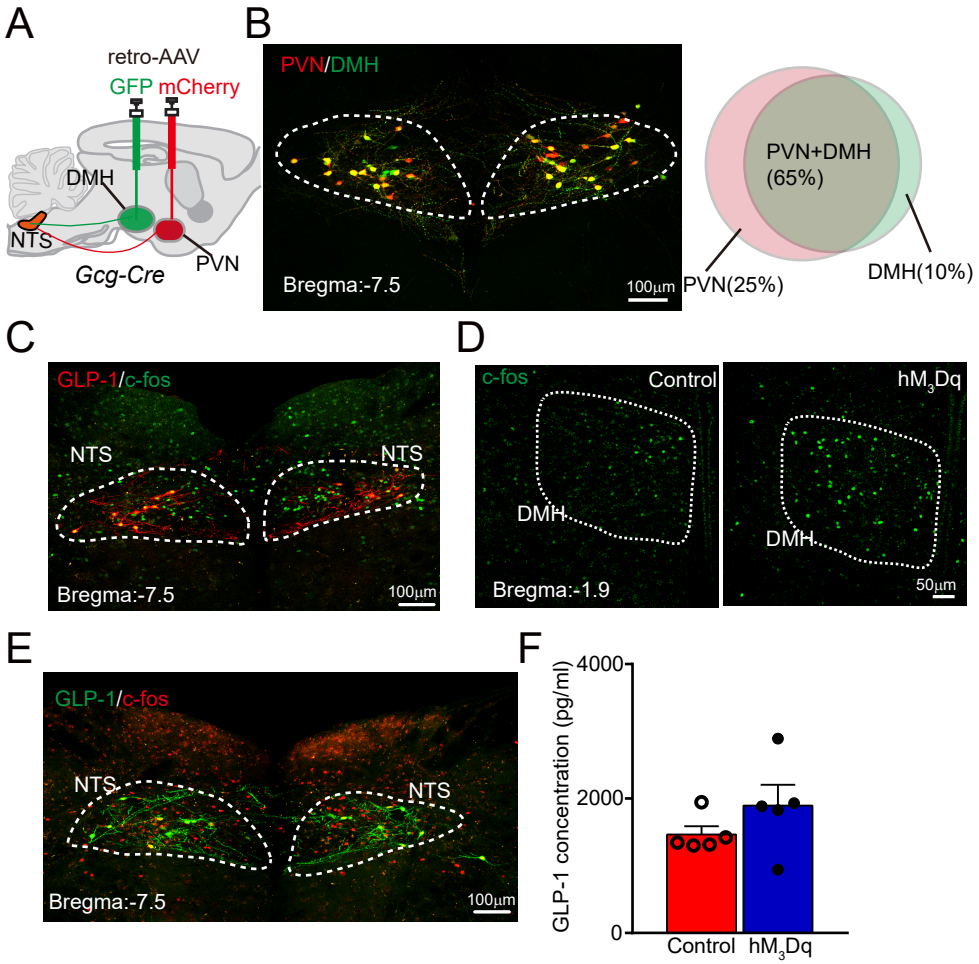

Figure S2| A, Experimental paradigm for retro-AAV viral injection in the PVN and DMH respectively of *Gcg-Cre* mice. **B**, Cre-dependent GFP expression in NTS demarks GLP-1 neurons which project to PVN (25%, mCherry), DMH (10%, GFP) and both PVN and DMH (65%, yellow). **C**, Cre-dependent hM3Dq expression in NTS of *Gcg-Cre* mice, which expressed c-fos after CNO injection. **D**, The representative image showed c-fos expression after chemogenetically activation of NTS GLP-1 neurons of *Gcg-Cre* mice. **E**, Cre-dependent retro-hM3Dq expression in NTS of *Gcg-Cre* mice, which expressed c-fos after CNO injection. **F**, GLP-1 concentration is showed in hM3Dq group than control group when chemogenetically activation of NTS GLP-1 neurons of Gcg-Cre mice ($p>0.05$, t-test).

Fig. S3.

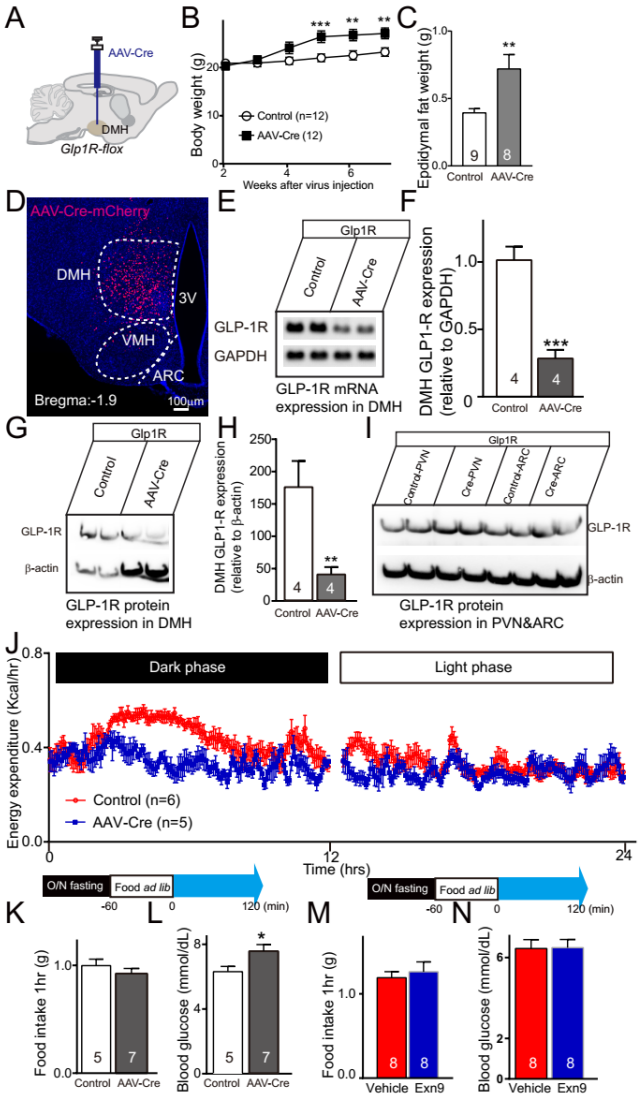

Figure S3|A, Experimental paradigm for viral injection of AAV-Cre in *GLP1R$^{f/f}$* mice; **B,** Body weight gain increased 5 weeks after depletion of DMH GLP-1R expression. ***p*<0.01, ****p*<0.001; **C**, Epididymal fat pad is heavier than control group, ** *p*<0.01 (t-test); **D**, AAV-Cre-mCherry virus expression pattern in the DMH in *GLP1R$^{f/f}$* mice; **E,** DMH brain slices were harvest freshly and mRNA was extracted immediately after. By using the GLP-1R specific primers, we did the quantitative PCR to analyze the mRNA expression. The representative gel bands showed GLP-1R expression are lower in AAV-Cre group (right two lanes) when compare to control group (left two lanes). **F,** Q-PCR results confirmed the knockout of GLP-1R expression in DMH , *** *p*<0.001 (t-test); **G&H,** We further confirmed the GLP-1R protein expression in DMH by western-blot. ** *p*<0.01 (t-test); **I**, GLP-1R expression was not changed in the PVN and ARC after depletion GLP-1R in the DMH. **J,** Energy expenditure analysis indicated that GLP-1R depletion mice showed lower energy expenditure in the dark period; **K,** In the postprandial glucose experiment setup, 1hr food intake amount was measured. There's no difference between control group and GLP-1R depletion group. While the baseline glucose level (t=-60min) was higher in GLP-1R depletion group when compare to control. **p*<0.05 (t-test) (**L**); Both 1hr food intake (t-test) (**M**) and baseline blood glucose level (t=-60min) (t-test) (**N**) were not different before Exn9 injection when investigating the GLP-1R antagonist-Exn9 effect on postprandial glucose (t-test).

Fig. S4.

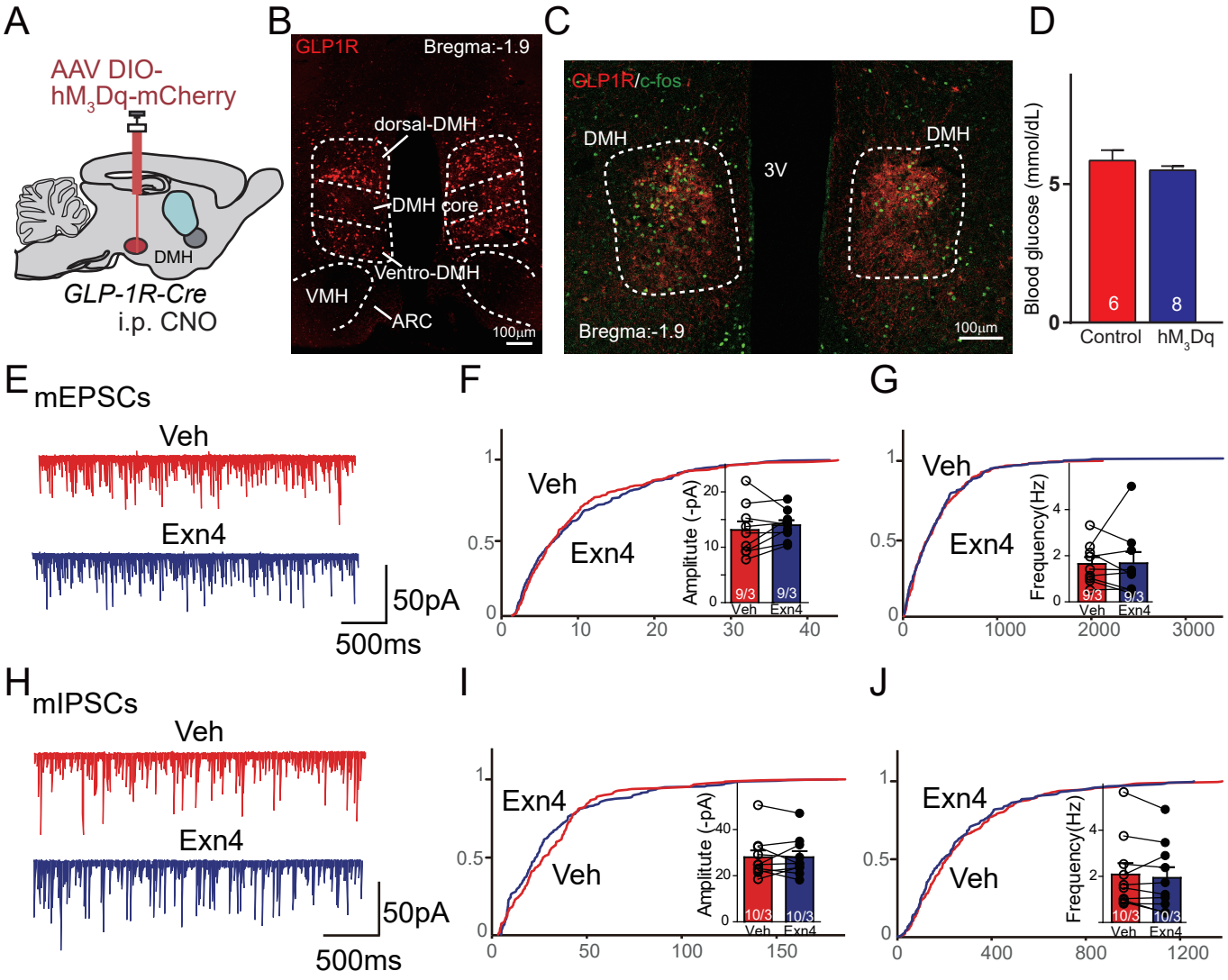

Figure S4| A, Experimental paradigm for viral injection in *GLP-1R-Cre* mice. **B**, AAV-DIO-mCherry expression in the DMH of *GLP-1R-Cre* mice.**C**, C-Fos expression in the GLP-1R neurons within the DMH after CNO injection in *GLP-1R-Cre* mice. **D**, Baseline glucose levels before CNOinjection (fasting condition) were not different (p>0.05, t-test); **E**, Representative trace for miniature-EPSC before and after Exn4 treatment inDMH GLP-1R neurons of *GLP-1R-Cre* mice. **F**, Cumulative amplitude probability plots of mEPSCs in typical DMH GLP-1R neurons before andafter Exn4 application. Inset in f: pooled data. n=9/3, cells/animals; p>0.05, paired t-test; **G**, Cumulative frequency probability plots of mEPSCsin typical DMH GLP-1R neurons before and after Exn4 application. Inset in g: pooled data. n=9/3, cells/animals; p>0.05, paired t-test. **H**, Representative trace for miniature-IPSC before and after Exn4 treatment in DMH GLP-1R neurons of GLP-1R-Cre mice. **I**, Cumulative amplitude probability plots of mIPSCs in typical DMH GLP-1R neurons before and after Exn4 application. Inset in i: pooled data. n=10/3, cells/animals; p>0.05, paired t-test; **J**, Cumulative frequecy probability plots of mIPSCs in typical DMH GLP-1R neurons before and after Exn4 application. Inset in j: pooled data. n=10/3, cells/animals; p>0.05, paired t-test. The data presenting style for panel E-J was adapted from our previous publication as described in main Figure2.

Fig. S5.

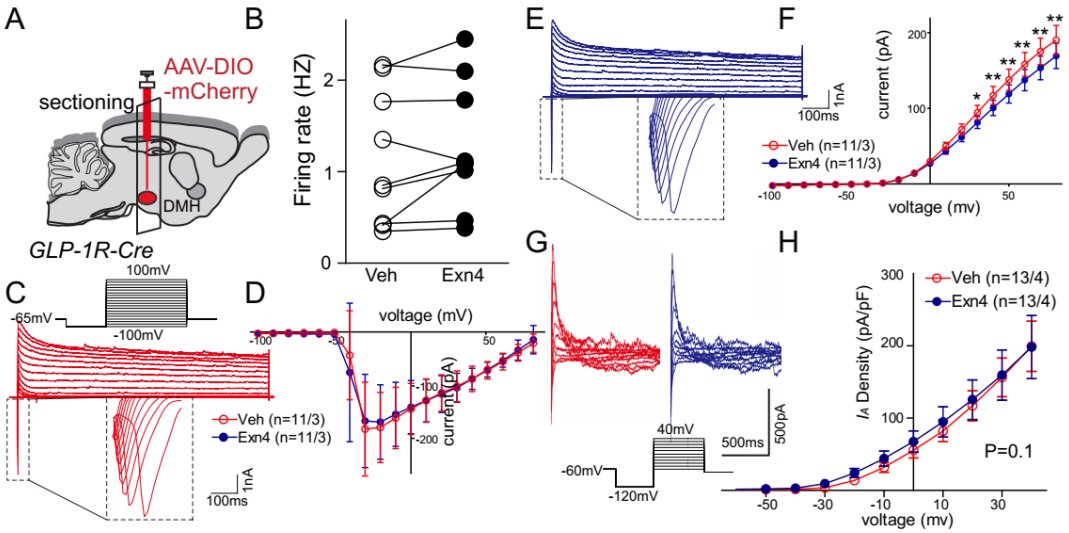

Figure S5| A, Experimental paradigm for recording GLP-1R positive neurons within DMH by injecting AAV-DIO-mCherry into *GLP-1R-Cre* mice; **B,** Action potential firing rate is not significantly changed when comparing vehicle group with Exn4 group. $p>0.05$ (paired t-test); **C&E,** Representative trace of voltage-step recording to isolate Na^+ and K^+ currents before and after treatment of GLP-1R agonist-Exn4; Exn4 did not alter voltage dependent sodium channel activity(**D**) but did change potassium channel activity (**F**) *$p<0.05$,**$p<0.01$ (repeat measurement, *post-hoc* pair-t-test); **G**, Representative trace and stimulation protocol for measurement of I_A before and after Exn4 treatment; **H,** I-V curve shows no significant shift after Exn4 treatment (repeat measurement, group effect $p>0.05$, group x voltage effect $p>0.05$);

Fig. S6.

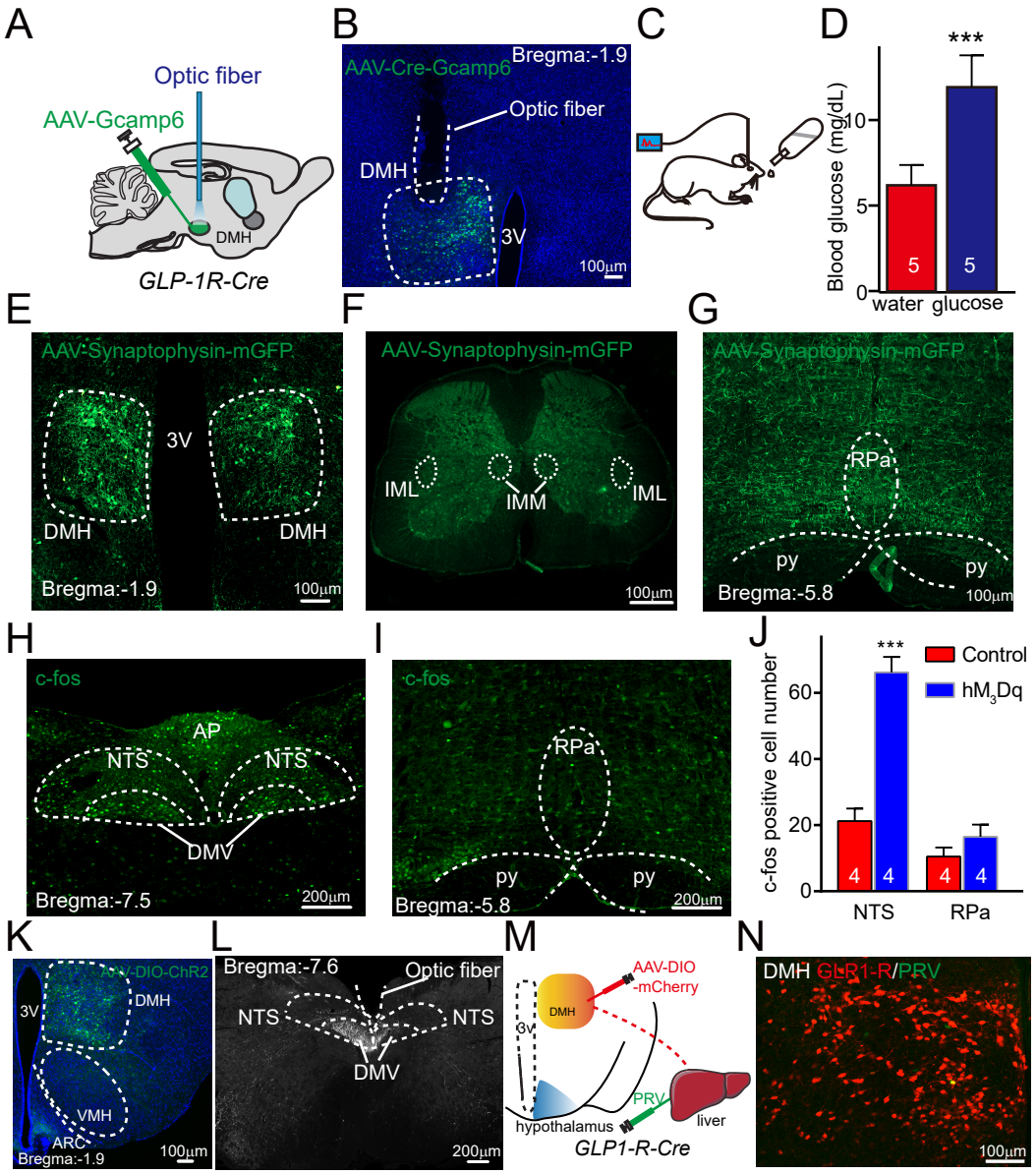

Figure S6| A, Experimental paradigm for investigation of in vivo Ca^{2+} image in the DMH of *GLP-1-R-Cre* mice. **B**, The expression of GCaMP6 and location for optic fiber; **C**, Experimental paradigm for fiber photometry recording in DMH during glucose uptake in *GLP-1R-Cre* mice. **D**, Blood glucose levels were significantly increased after 5min glucose uptake. ***p<0.001 (t-test) **E**, The expression of GFP after injection of AAV-DIO-synaptophysin-mGFP in DMH of *GLP-1R-Cre* mice; **F**, No GLP-1R afferents were observed in the IML region. **G**, Cre-dependent mGFP expression in the RPa originating from GLP-1R afferents. Chemogenetical stimulation of DMH GLP-1R neurons induced c-Fos expression in the NTS (**H**) and PRa (**I**) of *GLP-1R-Cre* mice. **J**, C-Fos positive cells are significantly higher in the NTS after CNO injection in the hM_3Dq group when compare to control animals (AAV-mCherry), but no in the RPa (*** p<0.001, t-test). **K**, Cre-dependent ChR2 expression in the DMH of *GLP-1R-Cre* mice. **L**, Location of optic fiber in the optogenetic experiment setup. **M**, Schematic showing tracing of DMH GLP-1R+ neurons-liver projection: PRV-GFPand AAV-DIO-mCherry were injected into liver and DMH respectively in *GLP-1R-Cre* mice; **N**, Representative imageshowing GLP-1R+ neurons (red) and liver projecting neurons (green). Py:pyramidal tract; RPa: raphe pallidus nucleus;IML:intermedio-lateral nucleus; IMM: intermedio-medial nucleus